RESEARCH ARTICLE

Preparation of expanded graphite composite membranes doped with oxidants and construction of their efficient wastewater degradation composite system

Xinyan Liu, Tong Liu*

School of Biomedical and Chemical Engineering, Liaoning Institute of Science and Technology, Benxi, Liaoning, China.

Received: December 10, 2025; **accepted:** April 27, 2026.

Efficient degradation of wastewater is crucial for addressing water pollution issues. Graphene oxide layered membranes can achieve molecular-level purification and are ideal materials for wastewater treatment. However, they easily expand in water, leading to a decrease in separation performance. To address this issue and achieve efficient wastewater degradation, this study investigated the preparation of graphene oxide by doping it with potassium permanganate as a strong oxidant. Six composite dispersions were prepared by adjusting the ratio of graphene oxide to polyvinyl alcohol. The final composite membranes were then obtained through pretreatment of the support, dip-coating, and borate ester crosslinking, thus completing the construction of a wastewater degradation composite system. Furthermore, several performance tests including apparent viscosity, wastewater degradation efficiency, and mechanical strength were designed to analyze the performance of the composite membranes under different ratio conditions. The results showed that the graphene oxide concentration 7.0mg/mL, polyvinyl alcohol concentration 1.9 mg/mL with a mass to volume ratio of approximately 3.68:1 composite membrane (G5) exhibited the best degradation effect on methyl orange and Congo red with degradation concentrations of 9.5 mg/L and 8.2 mg/L, respectively, after 15 hours. Simultaneously, its wastewater treatment flux after 48 hours was 13.5 L/m²·h with the smallest flux decrease. Its average tensile strength was 35.5 MPa, the water contact angle after crosslinking was 48.3 ± 0.5°, and its normalized flux after the sixth cycle in lysozyme solution was 72.6%. The results demonstrated that the composite membrane with a balanced ratio of graphene oxide and polyvinyl alcohol exhibited superior overall performance. This research provided experimental evidence and technical support for the development of efficient and stable wastewater treatment membrane materials.

Keywords: graphene oxide; wastewater degradation; polyvinyl alcohol; composite membrane; antifouling.

***Corresponding author:** Tong Liu, School of Biomedical and Chemical Engineering, Liaoning Institute of Science and Technology, Benxi, Liaoning 117004, China. Email: Ltong1007@163.com.

Introduction

Water pollution poses a significant and central challenge in the realm of global environmental governance with industrial dyeing and printing wastewater standing out as a particularly prominent issue. This type of wastewater contains persistent organic pollutants such as methyl orange and Congo red. If discharged directly without treatment, it will disrupt the ecological balance of aquatic bodies, leading to the death of aquatic organisms and even seeping

into the soil to pollute groundwater, ultimately threatening human drinking water safety and health [1, 2]. It is essential to develop efficient wastewater degradation technologies.

Currently, commonly used methods for addressing this problem include adsorption, biodegradation, and membrane separation technologies [3, 4]. Karthikeyan *et al*. used phthalic acid and 2-aminoterephthalic acid as ligands and introduced a solvothermal method to synthesize organic frameworks with different morphologies including one-dimensional rods, two-dimensional sheets, and three-dimensional particles. The results showed that the two-dimensional sheet morphology obtained a degradation rate (DR) close to 94% [5]. To improve the antifouling performance of membranes in membrane separation technology, Xia *et al*. prepared a high-performance catalyst with significant oxygen activation activity and integrated it onto the membrane surface through simple pump filtration, thereby obtaining a self-cleaning membrane with excellent antifouling ability. The results showed that the modified membrane exhibited excellent antifouling and filtration performance and had a stable structure [6]. Yi *et al*. used a high-temperature solid-state method to prepare a new photocatalyst containing strontium titanate, cobalt hydroxyoxide and aluminum, and introduced a reverse phase process to prepare a composite photocatalytic membrane. The results showed that, after running for 150 min, the rejection rate of the prepared membrane for Congo red reached 100% [7]. To efficiently treat emulsified oil wastewater, Tian *et al*. used ceramic membranes with strong antifouling properties, proposed the short-flow plate ceramic membrane process, and analyzed the characteristics of emulsified oil and the characterization performance of flat ceramic membranes. In addition, the optimal process conditions for treating emulsified oil wastewater were obtained by gel permeation chromatography. The results showed that the plate ceramic membrane could effectively retain emulsified oil and reduce the chemical oxygen demand in the water [8]. Current wastewater treatment solutions are quite diverse such as developing self-cleaning membranes and preparing composite photocatalytic membranes. However, current methods have certain problems such as the tendency of adsorption methods to generate secondary pollution and the tendency of graphene oxide layered membranes in membrane separation technology to swell in water, leading to a decrease in separation performance. Membrane separation technology relying on the selective permeability of membrane materials achieves precise separation of pollutants, demonstrating advantages such as outstanding purification efficiency, excellent energy consumption and environmental friendliness, and flexible operation and adaptability in wastewater treatment [9, 10]. Graphene oxide is a single-atom-layer two-dimensional nanomaterial prepared from graphite through processes such as oxidation and ultrasonic exfoliation. It can be made into separation membranes in the field of water treatment to achieve molecular-level purification [11]. Graphene oxide layered membranes relying on their unique structure formed by stacked layers have become ideal materials for wastewater treatment, exhibiting not only precise molecular sieving performance but also strong structural designability [12, 13]. However, there are still significant limitations such as their expansion tendency in water leading to a decrease in separation performance. To address this issue, polyvinyl alcohol was introduced to modify them, which possesses multiple advantages for membrane modification including excellent film-forming and adhesive properties, enhanced interlayer bonding, good environmental stability, improved swelling resistance of graphene oxide membranes, outstanding biocompatibility, preventing secondary pollution, and facilitating process control and shaping.

This study leveraged the advantages of membrane separation technology by employing graphene oxide layered membranes with an expansion tendency and introducing polyvinyl

alcohol to prepare a composite membrane (CM) to address the stability defects of pure graphene oxide membranes and develop efficient and anti-fouling wastewater treatment membrane materials. Simultaneously, a strong oxidant was added to enhance the degradation capacity of the CM. In addition, to solve the graphene oxide membrane swelling problem, this study adopted a "graphene oxide-polyvinyl alcohol composite + borate ester crosslinking" process and incorporated potassium permanganate as a strong oxidant to achieve functional synergy with graphene oxide. This design not only maintained the separation advantages of membrane materials in wastewater treatment but also endowed them with efficient degradation capabilities through the doping of oxidants. This research systematically explored the synergistic effect of the ratio on membrane performance and provided support for the development of wastewater treatment membranes.

Materials and methods

Preparation of graphene oxide/polyvinyl alcohol CM

1. Preparing graphene oxide

The study applied the graphene oxide polyvinyl alcohol composite + boronic ester crosslinking process and doped with potassium permanganate strong oxidant to prepare the composite film. The graphene oxide was prepared by using the Hummers method in a fume hood. Briefly, 2 g of graphite powder with the particle size less than 20 μm and carbon content ≥ 99.0% (China National Pharmaceutical Group, Shanghai, China) was placed in a 1,000 mL three necked flask and mixed with 46 mL of concentrated analytical grade sulfuric acid (mass fraction 98%) at 500 rpm for 30 minutes in a 0 - 5℃ ice water bath. 6 g of potassium permanganate (purity ≥ 99.5%) (Tianjin Fuyu Fine Chemical Co., Ltd., Tianjin, China) was slowly added and kept at ≤ 10℃ for continuing stirring for 2 hours. The water bath temperature was then raised to 35℃ and stirred at a constant temperature for 1 hour before slowly adding 92 mL of ultrapure water dropwise to the system and then raising the temperature to 98℃ and stirring at a constant temperature for 30 minutes. 5 mL of 30% hydrogen peroxide was then added and stirred for 10 minutes until no bubbles being generated to terminate the oxidation reaction. After the reaction system was cooled to room temperature, it was washed with 5% dilute hydrochloric acid and centrifuged at 8,000 rpm for 10 minutes for 3 times followed by washing with ultrapure water and centrifuged until the pH of the filtrate reaching approximately 7. The washed product was dispersed in ultrapure water and sonicated with a KQ-500DE ultrasonic generator (Kunshan Ultrasonic Instrument Co., Ltd., Kunshan, Jiangsu, China) for 30 minutes to obtain an aqueous dispersion of graphene oxide, which was sealed and stored for future use.

2. Preparing graphene oxide/polyvinyl alcohol composite dispersion solution

5 g of analytical grade polyvinyl alcohol with polymerization degree of 1,700 – 1,800 (China National Pharmaceutical Group, Shanghai, China) was placed in a 250 mL beaker and mixed with 95 mL of ultrapure water to prepare a 5% (w/w) polyvinyl alcohol aqueous solution at 90°C by magnetic stirring in a HH-S4 digital constant temperature water bath (Jincheng Guosheng Experimental Instrument Factory, Changzhou, Jiangsu, China) until completely dissolved before cooling down to room temperature. An appropriate amount of anhydrous ethanol was added to the previously prepared graphene oxide aqueous dispersion and sonicated for 30 minutes using an ultrasonic generator at a volume ratio of 1:4 between ethanol and graphene oxide dispersion. The prepared uniform graphene oxide aqueous dispersion was slowly added to 5% polyvinyl alcohol aqueous solution at different volume ratios and stirred at 1,000 rpm for 1 hour. Six sets of graphene oxide/polyvinyl alcohol composite dispersions with different ratios (g/mL) were then prepared as G1 (3.0/0.7), G2 (5.0/1.3), G3 (5.0/1.9), G4 (7.0/1.3), G5 (7.0/1.9), G6 (9.0/2.5), respectively. The dispersions were stood for 10 minutes to remove bubbles and sealed for later use.

3. Pretreatment of the supporting carrier

50 μm pore size qualitative filter paper (Zhenkunxing Industrial Supermarket, Shanghai, China) was cut into rectangular pieces with the measuring of 2 cm × 5 cm and soaked in anhydrous ethanol for 15 minutes before being removed and rinsed for three times with ultrapure water. The filter paper was placed in a DGG-9030B electric constant temperature drying oven (Shanghai Senxin Experimental Instrument Co., Ltd., Shanghai, China) and dried at 60℃ for 2 hours until constant weight being reached. The prepared filter paper was sealed and stored for future use.

4. Preparing graphene oxide/polyvinyl alcohol composite film

The pretreated qualitative filter paper carrier was fully immersed in the graphene oxide/polyvinyl alcohol composite dispersion liquid for 10 minutes before being removed and drained the excess liquid on the surface. The filter paper was then placed in an electric constant temperature drying oven at 80℃ for 1 hour to form an initial graphene oxide/polyvinyl alcohol composite film layer.

5. Boronic ester crosslinking modification

5 g of boric acid was mixed with 95 mL of ultrapure water to prepare a 5% (w/w) boric acid crosslinking solution. The initial composite film was fully immersed in boric acid crosslinking solution at room temperature for 12 hours. After crosslinking was completed, the composite film was removed and rinsed with ultrapure water for 15 minutes to remove boric acid and impurities.

6. Complete drying and sealing molding

The washed composite film was placed in a DZF-6050 vacuum drying oven (Shanghai Yiheng Scientific Instrument Co., Ltd., Shanghai, China) at 60℃ and 0.08 MPa for 12 hours until constant weight was reached. The dried composite film was then sealed in a dryer to obtain the graphene oxide/polyvinyl alcohol oxide doped composite film (G1 - G6).

Performance tests of graphene oxide/polyvinyl alcohol CMs for wastewater degradation

1. Apparent viscosity test

Different mass ratios of graphene oxide/polyvinyl alcohol at 0.0, 0.1, 0.2, 0.3, 0.4, and 0.5 were tested under a 6 mg/mL pure graphene oxide dispersion. The apparent viscosity of the graphene oxide dispersion and the graphene oxide/ polyvinyl alcohol composite dispersion at different graphene oxide concentrations was analyzed.

2. Wastewater degradation performance test

Six time points of 0, 3, 6, 9, 12, and 15 hours were tested. The pollutants involved were methyl orange and Congo red with an initial concentration of 100 mg/L for all cases.

3. Degradation rate (DR) test

In the test of the DR change of the CM, the initial concentration of pollutants was set to 100 mg/L. The concentrations of pollutants at 1, 3, 6, 9, 12, and 15 hours were recorded simultaneously. The instantaneous DR at each time point was calculated as follows [16-18].

$$u = \frac{C_0 - C_t}{t} \quad (1)$$

where u was the DR (mg/L·h). C_0 was the initial concentration of pollutants (mg/L). t was the reaction time (h). C_t was the concentration of pollutants at time t (mg/L).

4. Membrane reusability test

The process of each use was degradation for 6 h → ultrapure water rinsing for 15 min → degradation again, which was repeated 5 times. The DR corresponding to these 5 times was recorded. The DR (R) was calculated as below [19].

$$R = \frac{C_0 - C_6}{C_0} \quad (2)$$

where C_6 was the pollutant concentration after 6 hours of degradation (mg/L).

5. Membrane anti fouling performance test

The study continuously treated actual wastewater from a dyeing and printing plant and recorded the flux and flux decrease at 8, 16, 24, 32, 40, and 48 hours.

6. Mechanical strength test of CM

The CMs of groups G1 - G6 were cut into "dumbbell-shaped" 20 mm × 5 mm with three parallel samples per group. The tensile strength and elongation at break were tested. The tensile strength σ was calculated as follows.

$$\sigma = \frac{F}{A} \quad (3)$$

where F was the max tensile force (N). A was the cross-sectional area of the specimen (mm^2). The calculation of the elongation at break ε was shown below.

$$\varepsilon = \frac{L - L_0}{L_0} \times 100\% \quad (4)$$

where L was the length of the sample at break (mm). L_0 was the initial length of the sample (mm).

7. Hydrophilicity test of CM

The water contact angles of each CM before and after crosslinking were recorded by using a Theta Flex contact angle measuring instrument.

8. Pollution (fouling) resistance test

Bovine serum albumin solution and lysozyme solution were prepared with ultrapure water, both with a concentration of 1 g/L. The process of each cycle was filtering the contaminated liquid for 30 min before rinsing with ultrapure water for 15 min followed by testing the pure water flux. A total of 6 cycles were performed. The standardized flux f calculation for each cycle was shown below [20].

$$f = \frac{J_t}{J_0} \times 100\% \quad (5)$$

where J_t was the pure water flux after each cycle flushing ($L/m^2 \cdot h$). J_0 was the initial pure water flux ($L/m^2 \cdot h$).

Statistical analysis

All experimental data were analyzed and processed by using SPSS 26.0 statistical software (IBM, Armonk, NY, USA). The comparison of differences between groups was conducted by using one-way ANOVA. If the variance was homogeneous, LSD method was used for multiple comparisons. If the variance was heterogeneous, Dunnett's T3 method was used. The experimental results were expressed as mean ± standard deviation with *P* value less than 0.05 indicating statistical significance and *P* value less than 0.01 indicating extremely significant statistical significance.

Results and discussion

Analysis of apparent viscosity

The apparent viscosity test results of different dispersions showed that the viscosity gradually increased with the increase of the graphene oxide/polyvinyl alcohol mass ratio from 357 mPa·s to 1,482 mPa·s (Figure 1a). The apparent viscosity of the G5 composite dispersion demonstrated extremely significant difference from that of G1, G2, and G3 groups ($P < 0.01$), and showing the significant difference compared to that of G4 and G6 groups ($P < 0.05$). The results indicated that there was an interaction between graphene oxide and polyvinyl alcohol. With the increase of graphene oxide content, the stacking and entanglement of graphene oxide sheets in the composite dispersion intensified, and the intermolecular forces were strengthened, thus the viscous flowability of the system increased. When the graphene oxide concentration increased, the apparent viscosity of both the graphene oxide dispersion and the graphene oxide/polyvinyl alcohol composite dispersion also increased synchronously with the graphene oxide/polyvinyl alcohol composite dispersion increasing faster than that of graphene oxide

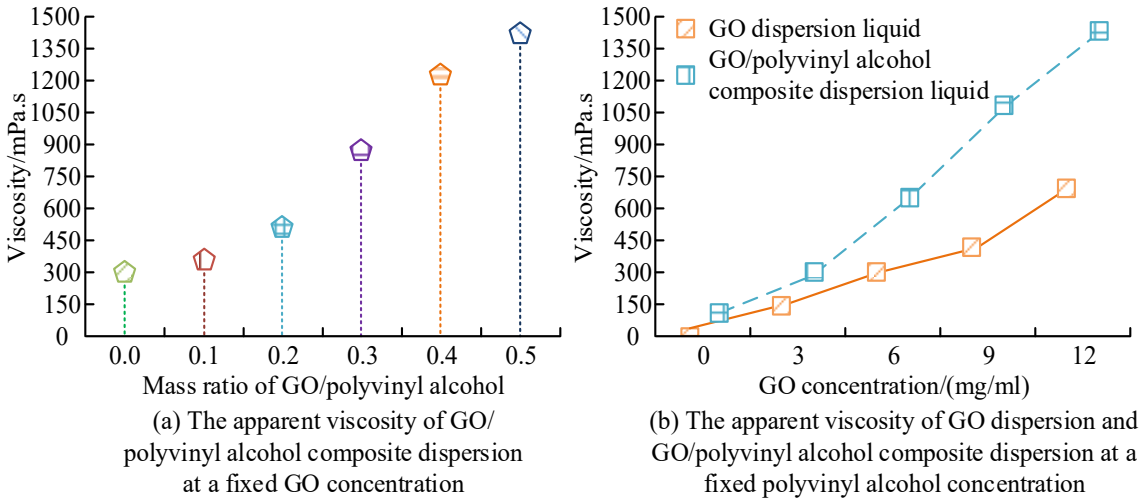

Figure 1. Apparent viscosity test results of different dispersion solutions.

dispersion. The maximum apparent viscosity values of the graphene oxide dispersion and the graphene oxide/polyvinyl alcohol composite dispersion reached 713.59 mPa·s and 1,429 mPa·s, respectively (Figure 1b). The viscosity increase of the graphene oxide/polyvinyl alcohol composite dispersion was significantly higher than that of the pure graphene oxide dispersion, indicating that polyvinyl alcohol could enhance the interlayer interaction of graphene oxide sheets. The addition of polyvinyl alcohol significantly improved the sensitivity of the dispersion to changes in graphene oxide concentration. Its molecular chains could form hydrogen bonds and other interactions with the oxygen-containing functional groups on the surface of graphene oxide sheets, further promoting the uniform dispersion and network construction of graphene oxide sheets. The results laid a better foundation for the preparation of structurally stable graphene oxide/polyvinyl alcohol CMs.

Analysis of wastewater degradation performance

The wastewater degradation results of different CMs demonstrated that the methyl orange degradation concentrations of different CMs gradually decreased with increasing time, and the methyl orange degradation concentration of the G5 CM was the lowest, reaching 9.5 mg/L at 15 h. In wastewater treatments, the degradation concentrations of methyl orange by different CMs after 15 h were 36.5, 28.7, 20.8, 15.2, 9.5, and 11.2 mg/L for G1, G2, G3, G4, G5, and G6, respectively (Figure 2a). The degradation concentration of methyl orange in G5 group was significantly different from those in G1, G2, G3, G4, and G6 groups ($P < 0.01$). Furthermore, after 48 h of continuous wastewater treatment, the G5 membrane consistently exhibited the highest flux, and its flux decrease was significantly less than other CMs, demonstrating superior antifouling performance. The results indicated that the G5 CM had a superior degradation effect on methyl orange and a better degradation effect compared to the other membranes. The Congo red degradation concentration of the G5 CM was lower than the others at all time points. The degradation concentration of Congo red in the G5 group was significantly lower than that in G1, G2, G3, G4, and G6 groups ($P < 0.01$) (Figure 2b). The results indicated that G5 CM exhibited a significant advantage in the degradation of Congo red, and this degradation advantage remained stable at different stages over time. The G5 CM demonstrated good degradation performance for both methyl orange and Congo red.

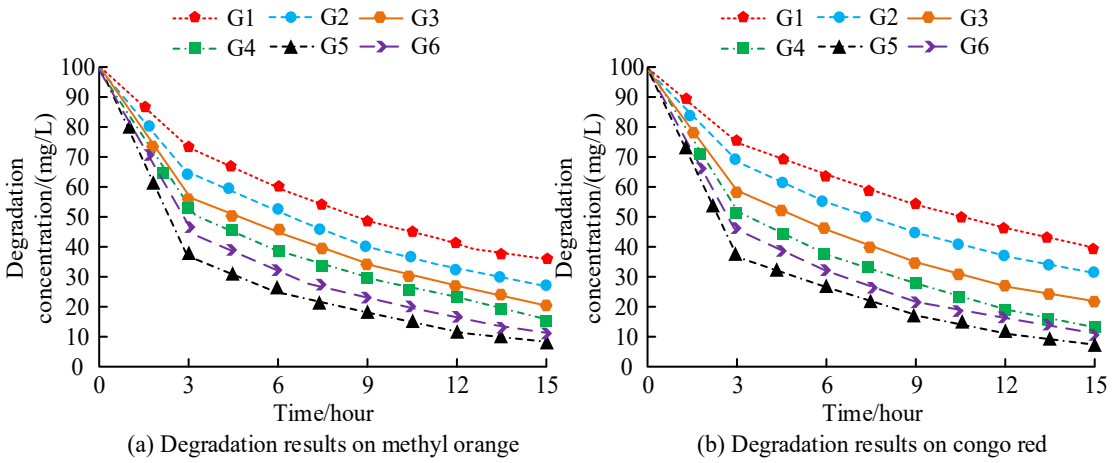

Figure 2. Wastewater degradation results of different CMs.

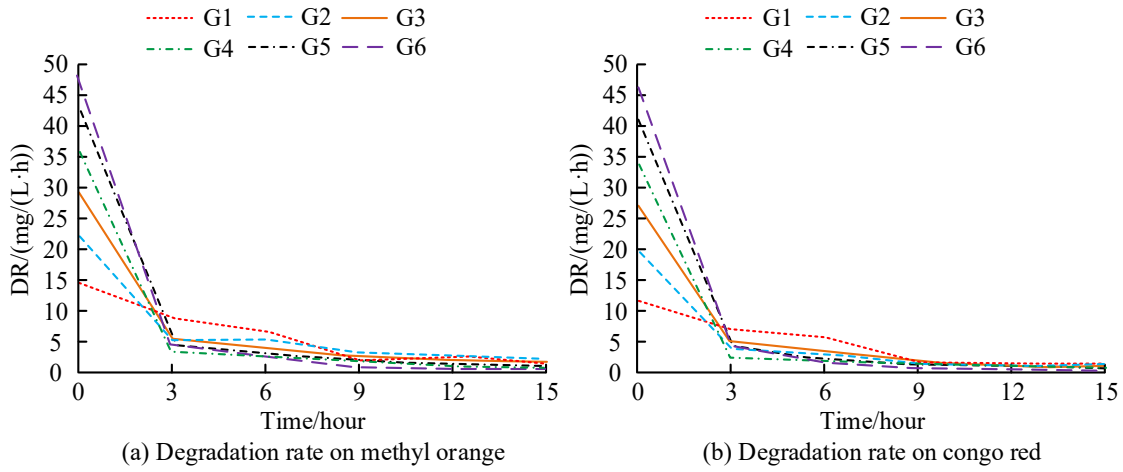

Figure 3. Changes in degradation rates of different composite films.

Analysis of DR changes

The changes in DRs of different CMs showed that the DR of methyl orange by different CMs decreased with increasing time. At 3 h, the DR of G4 was the lowest ($P < 0.01$), while from 6 h to 15 h, the DR of G6 was the lowest, while the DR of methyl orange in G5 group was significantly different from those in G1, G2, and G3 groups ($P < 0.01$) (Figure 3a). The results indicated that the DR of methyl orange by the CMs was affected by the reaction time and the graphene oxide/polyvinyl alcohol ratio in the membrane. Different membrane ratios showed differences in the utilization efficiency and stability of active sites, generally conforming to the pattern of high rate in the early stage of the reaction and slowing down in the later stage due to the reduction of substrate. The minimum DR at different time points for Congo red was consistent with that of methyl orange. At 15 h, the DRs corresponding to G1 to G6 CMs were 1.21, 0.93, 0.82, 0.78, 0.69, and 0.54 mg /(L·h), respectively, which indicated that the degradation pattern of Congo red by the CM was consistent with that of methyl orange, and the material ratio had a common effect on the DR of different dyes. At 6-15 hours, the DR of Congo red in G6 group was significantly different from those in G5 group ($P < 0.05$), while, at 15

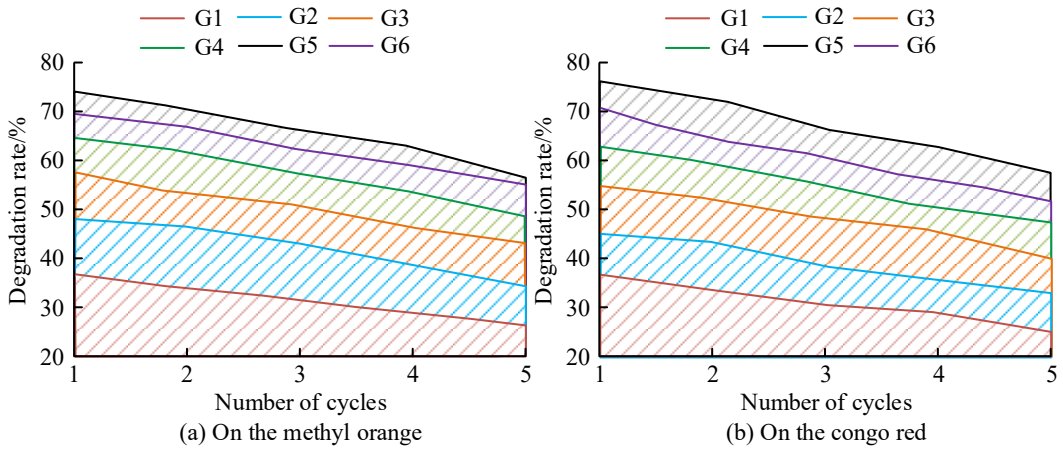

Figure 4. Performance analysis of membrane reuse.

hours, the DR of Congo red in the G5 group was significantly different from those in G1, G2, and G3 groups ($P < 0.01$) (Figure 3b). All membranes showed low DRs after 15 hours. The results suggested that the DR of the two dyes by the expanded graphite-based CM was affected by the material ratio and time.

Analysis of membrane reuse and membrane antifouling performance

The membrane reuse performance analysis demonstrated that, on methyl orange, the DR of all CMs gradually decreased with increasing cycle number, but the cycle stability of CMs with different ratios showed significant differences. Among them, the G5 CM had the highest initial DR of 74.4% and remained at a high level of 57.8% after 5 cycles. The G1 CM performed the worst with a DR of 26.5% after 5 cycles (Figure 4a), which was because, in the high graphene oxide concentration CM, the graphene oxide sheets and polyvinyl alcohol crosslinked through borate esters to form a more stable 3D network structure that could effectively desorb residual methyl orange during ultrapure water rinsing and reduce the blockage of active sites. In contrast, the low graphene oxide concentration CM had a lower degree of crosslinking and insufficient membrane structure stability, resulting in more significant loss of active sites after multiple cycles. On Congo red, the cycle degradation pattern of the CMs was highly consistent with that of the methyl orange. After 5 cycles, the DRs of G1 to G6 CMs were 25.0, 32.5, 40.8, 48.5, 57.2, and 53.8%, respectively (Figure 4b). G5 exhibited superior cycling stability in the degradation of both methyl orange and Congo red. After 5 cycles, the DRs of methyl orange and Congo red in the G5 group showed a highly significant statistical difference ($P < 0.01$) compared to the G1, G2, G3, and G4 groups, and a statistically significant difference ($P < 0.05$) compared to the G6 group. The membrane's antifouling performance analysis showed that, in the performance changes of different CMs continuously treating actual wastewater for 48 hours, the flux of different CMs decreased synchronously with the increase of time, and the flux of the G5 CM was consistently greater. The results showed that, at 48 hours, the flux of the G5 CM was 13.5 L/(m²·h), while the fluxes of the other CMs were 9.0 L/(m²·h), 10.6 L/(m²·h), 9.1 L/(m²·h), 12.2 L/(m²·h), and 11.2 L/(m²·h), respectively, for G1, G2, G3, G4, and G6 (Figure 5a). At different times, the flux decrease of the G5 CM was the smallest, while the flux decrease of the G1 CM was the largest (Figure 5b). The results showed that all different CMs had good wastewater treatment effects. Among them, the G5 CM, due to its balanced ratio of graphene oxide and polyvinyl alcohol, not only maintained a high flux throughout 48 hours of continuous

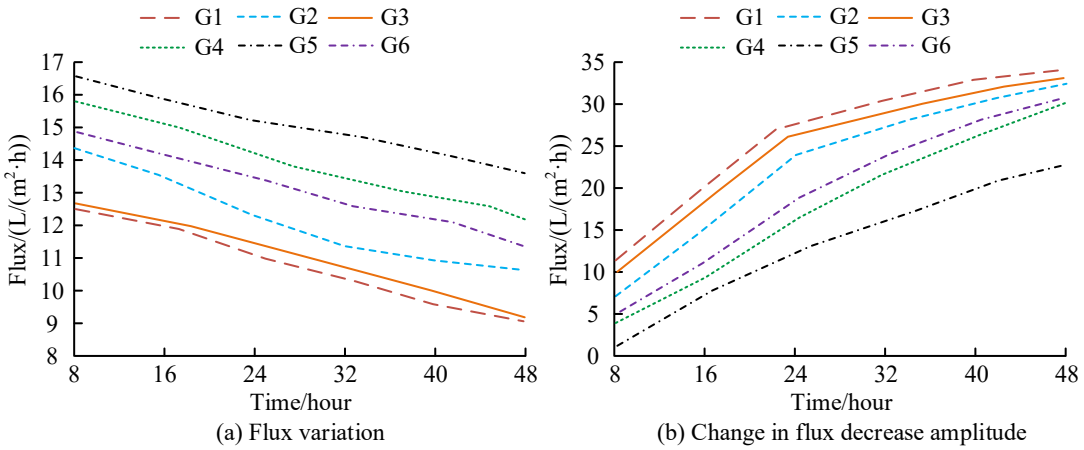

Figure 5. Analysis of membrane anti fouling performance.

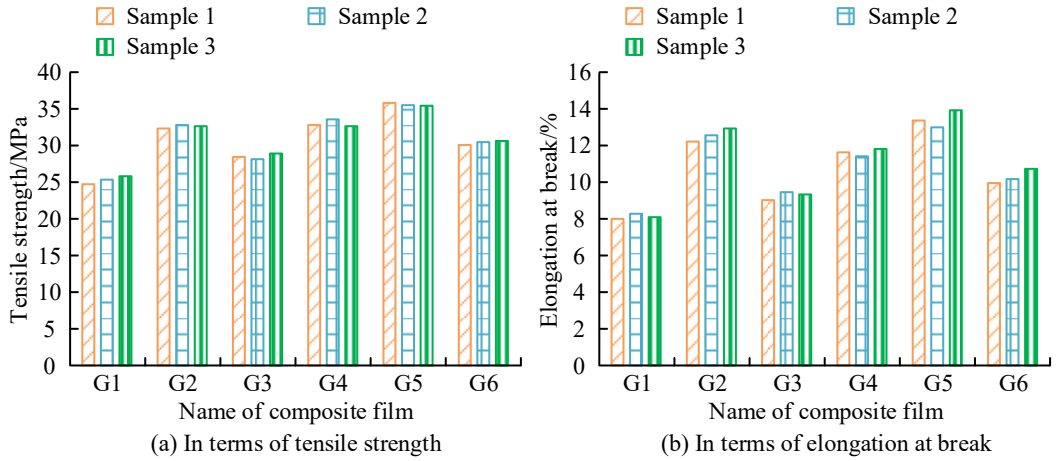

Figure 6. Analysis of mechanical strength results of different composite films.

treatment of actual wastewater but also had the smallest flux decline and the best antifouling performance, making it more suitable for long-term wastewater treatment. At 48 hours, the difference in wastewater treatment flux between the G5 group and the G1, G2, G3, G4, and G6 groups was highly significant and statistically significant ($P < 0.01$). The decrease in flux in the G5 group was significantly different from that in the G1, G2, G3 groups ($P < 0.01$), and G4 and G6 groups ($P < 0.05$).

Analysis of mechanical strength, hydrophilicity, and fouling resistance of the CM

The mechanical strength of different CMs demonstrated that the three parallel samples of each CM group showed very small deviations in tensile strength, indicating high repeatability and reliability of the experimental preparation process and testing operation. G5 exhibited the highest strength with an average value of 35.5 MPa, while G1 showed the lowest strength with an average value of 25.3 MPa (Figure 6a). The average elongation at break of the CMs in groups G1 to G6 were 8.13, 12.60, 9.33, 11.53, 13.57, and 10.27%, respectively (Figure 6b). The CM of G5 exhibited better mechanical strength because its graphene oxide and polyvinyl alcohol concentrations were balanced, which formed a

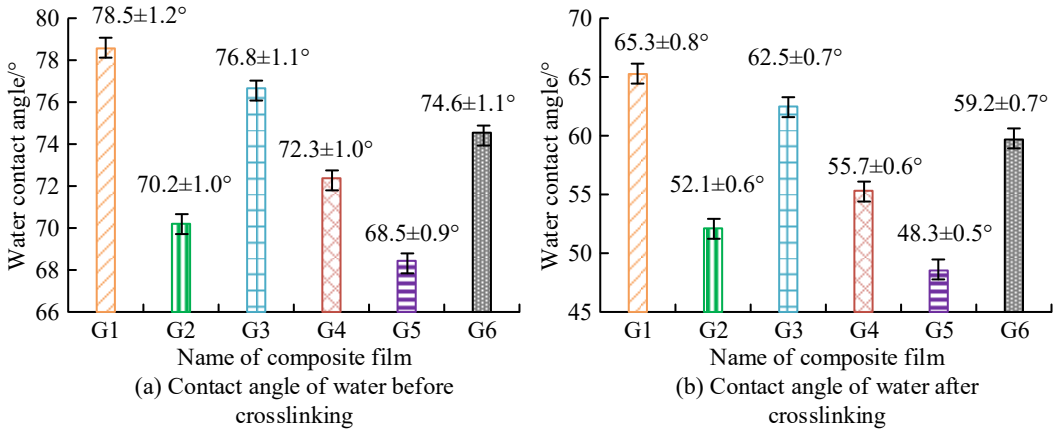

Figure 7. Hydrophilicity analysis of different CMs.

more stable three-dimensional network structure through borate crosslinking and enhanced the layer bonding force while retaining appropriate flexibility. The average tensile strength of G5 showed a highly significant statistical difference compared to G1, G2, and G3 (P < 0.01), while there was no significant statistical difference compared to G4 and G6. The elongation at break of G5 showed a highly significant statistical difference compared with G1, G3, and G6 (P < 0.01), while there was no significant statistical difference compared with G2 and G4. The hydrophilicity analysis of different CMs showed that, before crosslinking, the water contact angles of CMs G1 to G6 were all at a relatively high level with some differences among the different CMs. CM of G1 had the largest water contact angle at 78.5 ± 1.2°, indicating the weakest hydrophilicity, while CM of G5 had the smallest water contact angle at 68.5 ± 0.9°, indicating the better hydrophilicity than the other CMs before crosslinking (Figure 7a). After crosslinking, the water contact angles of all CMs decreased significantly compared to that before crosslinking, and the hydrophilicity of all membranes was improved. CM of G5 also had the smallest water contact angle after crosslinking at 48.3 ± 0.5°, indicating the best hydrophilicity. Moreover, the relative order of the water contact angles of each CM after crosslinking was consistent with that before crosslinking, further verifying that the crosslinking reaction between boric acid and polyvinyl alcohol hydroxyl groups could effectively increase the density of hydrophilic groups on the membrane surface, thereby improving hydrophilicity. The results also showed that the effect of different graphene oxide to polyvinyl alcohol ratios on the hydrophilicity of CMs was continuous. Regarding hydrophilicity, the water contact angles of all CMs decreased significantly compared to the uncrosslinked membranes, indicating improved hydrophilicity, which was particularly evident in G5 CM, where the water contact angle changed from 68.5 ± 0.9° to 48.3 ± 0.5° (Figure 7b). Such result suggested that the CM with a balanced graphene oxide to polyvinyl alcohol ratio effectively addressed the swelling problem of pure graphene oxide membranes. The difference in water contact angle before crosslinking between G5 and G1, G2, G3, G4, and G6 was statistically significant (P < 0.05), while the difference in water contact angle after crosslinking between G5 and G1, G2, G3, G4, and G6 was highly significant (P < 0.01). The difference in water contact angles before and after cross-linking in all groups was highly statistically significant (P < 0.01). The stain resistance analysis of different CMs showed that, in bovine serum albumin solution, the standardized flux of different CMs decreased with increasing cycle number. Furthermore, at different cycle numbers, the standardized flux of G5 CM was significantly better than that of other

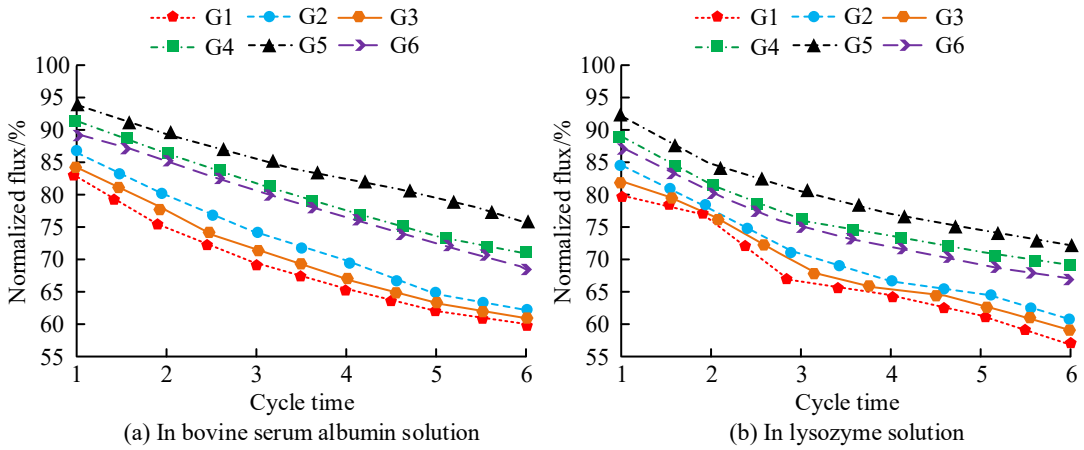

Figure 8. Analysis of pollution resistance of different composite films.

CMs. The results showed that, after the sixth cycle, the standardized flux of G5 CM was 77.2%, while the values for other CMs were all below 75% (Figure 8a). In lysozyme solution, G5 CM again performed better with a standardized flux of 72.6% after the sixth cycle, while the other CMs were all below 70% (Figure 8b). G5 CM exhibited superior fouling resistance, providing performance support for the long-term stable treatment of wastewater containing protein-containing pollutants. In both bovine serum albumin and lysozyme solutions, the normalized flux of G5 after the sixth cycle was significantly different from that of G1, G2, G3, G4, and G6 ($P < 0.01$).

This study still had some limitations as it only tested two simulated pollutants (methyl orange and Congo red) and a single type of dyeing and printing wastewater without exploring the degradation effect of the CM on various complex real-world wastewaters. Future research could expand the range of pollutants and wastewater types to verify the applicability of the CM in multi-component pollutant systems.

Acknowledgements

The research was supported by 2024 Liaoning Provincial Department of Education research team project (Grant No. 2024JYTKYTD-13, LJ222411430018, LJ232411430002), 2025 Liaoning Provincial Department of Education research team project (Grant No. LJ222511430002, LJ222511430002), 2026 Liaoning Institute of Science and Technology College Student Innovation and Entrepreneurship Training Program (Grant No. D202507080828447307).

References

1. Elmourabit M, Khaddoudi I, Allaoui I, Zarki Y. 2025. Preparation and application of nano-carbonated hydroxyapatite materials derived from phosphate sludge waste for photocatalytic degradation of dye pollutant. Ceram Int. 51(19):27208-27218.
2. Osman H, Yilmaz SI, Ugurlu M, Vaizogullar AI. 2025. Synthesis and characterisation of activated carbon supported catalysts: Photocatalytic degradation of olive wastewater solutions using these catalysts. J Sol-Gel Sci Technol. 115(3):1428-1448.
3. Permana I, Sudirja R, Jupesta J. 2023. Potential of vermifiltration technique to reduce chemical oxygen demand, biological oxygen demand, and total suspended solid of farm dairy effluent in developing countries: Case of Indonesian farm dairy industry. Green Low-Carbon Econ. 2(3):193-200.
4. Wang ZY, Yuan JX, Fang W, Chen H. 2025. Construction of carbon foam/g-C_3N_4 photothermal-photocatalytic synergistic evaporator for evaporation and degradation performance of wastewater. J Mater Eng. 53(8):129-139.
5. Karthikeyan G, Mohan S, Balakrishna RG. 2025. Multidimensional nickel-based nanoporous metal-organic framework-integrated photoactive membranes for pollutant separation and degradation in wastewater treatment. ACS Appl Nano Mater. 8(25):12966-12979.
6. Xia GJ, Zhou M, Shao WJ, Adeli M. 2025. Self-cleaning antifouling membrane engineered by oxygen-activated mof-

derived catalysts for efficient organic wastewater treatment. ACS Appl Mater Interfaces. 17(7):10637-10649.
7. Yi LD, Zhang Y, Xie YP, Zhang BG. 2025. High-efficiency $SrTiO_3$Al/CoOOH-PSF/PVDF photocatalytic membrane for synergistic degradation of organic pollutants. Res Chem Intermed. 51(9):5269-5286.
8. Tian Y, Liu FY, Shi MA, Wang XL, An FQ. 2025. Treatment of wastewater containing emulsified oil using flat ceramic membranes. J Ceram. 46(1):167-174.
9. Lang MJ, Yang ZM, Zeng GY. 2024. Construction of photocatalytic membrane separation materials and its research progress in wastewater treatment. Ind Water Treat. 44(7):47-56.
10. Zhang SD, Zhang XW, Shen X, Lu XR. 2025. Research status of membrane separation technology in the treatment of antibiotic wastewater. Environ Sci Water Res Technol. 11(6):1386-1400.
11. Mohammed MN, Aljibori HSS, Jweeg MJ, Al Oqaili. 2024. A comprehensive review on graphene oxide based nanocomposites for wastewater treatment. Pol J Chem Technol. 26(1):64-79.
12. Xue Y, Zhang CJ, Li SB, Zhou Q. 2024. Enhanced denitrification by graphene oxide-modified cathode for the secondary effluent of wastewater treatment plants in three-dimensional biofilm electrode reactors. Water Sci Technol. 89(12):3192-3207.
13. Kazemi N, Rezai B, Hoseinian FS. 2025. Recycling of graphene oxide nanocollector used in ion flotation for reusing in the wastewater treatment. Sep Sci Technol. 60(7):774-785.
14. Rout DR, Jena HM. 2023. Synthesis of graphene oxide-modified porous chitosan cross-linked polyaniline composite for static and dynamic removal of Cr(VI). Environ Sci Pollut Res. 30(9):22992-23011.
15. Duan CQ, Ren J, Tao L. 2023. Study on preparation of nanometer graphite oxide composites and treatment of heavy metal wastewater. J Funct Mater. 54(12):12085-12090.
16. Zhao MY, Luo XZ, Li D, Dong YQ. 2025. Monitoring the interfacial polymerization and membrane fouling of selective layer with boronate ester linkages via aggregation-induced emission. Chin J Polym Sci. 43(9):1505-1515.
17. Park G, You D, An J, Choi S. 2024. Boronic ester crosslinked gels for high strain rate stress wave attenuation. Compos Res. 37(6):441-446.
18. Vitezova M, Joksic T, Dordevic D, Vitez T. 2025. Aerobic and anaerobic microbial degradation in the wastewater treatment process affected by the presence of biodegradable packaging material made from plant by-products. Polym Bull. 82(11):5879-5907.
19. AlWafi R, Hammad MS, Mansour SF. 2024. Superior dye degradation for wastewater treatment based on nanocomposites of cerium oxide, gadolinium oxide and graphene oxide. Ceram Int. 50(10):16736-16746.
20. Liu Y, Rohwerder T, Bonatelli ML, von Postel. 2024. A novel sulfatase for acesulfame degradation in wastewater treatment plants as evidenced from *Shinella* strains. Environ Sci Technol. 58(42):18892-18902.